

# Results on Self-sensing Active Magnetic Bearings

(\*) Alexandre Schammass, (\*\*) Hannes Bleuler

(\*) Laboratoire de systèmes robotiques, EPFL, Lausanne, Switzerland  
+41 21 693 5958 / +41 21 693 3810, [alexandre.schammass@epfl.ch](mailto:alexandre.schammass@epfl.ch)

(\*\*) Laboratoire de systèmes robotiques, EPFL, Lausanne, Switzerland  
+41 21 693 5927 / +41 21 693 3810, [hannes.bleuler@epfl.ch](mailto:hannes.bleuler@epfl.ch)

## Acknowledgments

The authors would like to thank the Kommission für Technologie und Innovation (KTI) for the financial support of this research project.

## Keywords

active magnetic bearings, position estimation, switching amplifier, self-sensing bearings.

## Abstract

Self-sensing active magnetic bearings eliminate the position sensors and estimate the position of the levitated object position by measuring the coil current and voltage. The main interest of this approach is to reduce production costs and hardware complexity. This paper proposes a strategy for estimating the position based on a modulation approach. Experimental results from a radial magnetic bearing are presented. The quality of the estimation signal is evaluated in terms of noise and dynamic performance (bandwidth).

## 1 Introduction

Due to its contact-free suspension, active magnetic bearings (AMBs) have a number of advantages over conventional bearings. These advantages include elimination of lubrication, friction-free operation and capability of operation at higher speeds. For this reason, AMBs could be used in applications with high rotor speeds and high power density.

In the recent years, magnetic bearing technology created an industrial breakthrough in the field of high vacuum technology (turbo-molecular pumps) and turbo machines (compressor/expander). At present, the worldwide total number of the sold AMBs lies over 50,000 pieces and its market is increasing rapidly. For this growth, it is important that the magnetic bearing technology can be applied in new fields like air conditioning, fuel cells, and cogeneration. These new applications have a potential of large production (10,000 to 100,000 pieces/year). In order to achieve this production, the AMB system has to be:

- More compact (less components)
- Substantially cheaper.
- More reliable.

An AMB consists of electromagnetic coils, an automatic controller and discrete position sensors. The idea of the self-sensing AMB is to eliminate the position sensors and to estimate the position by measuring the current of the actuator coils. This represents a significant cost reduction. The additional advantages are a reduced the number of components, an increased system reliability and a shorter rotor (i.e. higher structural frequencies).

This paper presents a self-sensing AMB based on amplitude modulation approach. The paper is organized as follows: Section 2 shows the types of self-sensing AMBs. Section 3 presents the model of the coil and the PWM amplifier. In Section 4, the position estimation algorithm is proposed. Section 5 shows experimental results from one axis of a radial bearing.

## 2 Types of Self-Sensing Active Magnetic Bearings

As shown in Figure 1, the approaches for self-sensing AMBs can be divided in two classes: Linear control and modulation approaches. Linear control approach [1, 2] is based on the fact that one system is observable only having the current as output, and then the position is estimated by using a linear state estimator as observer (according to Luenberger).

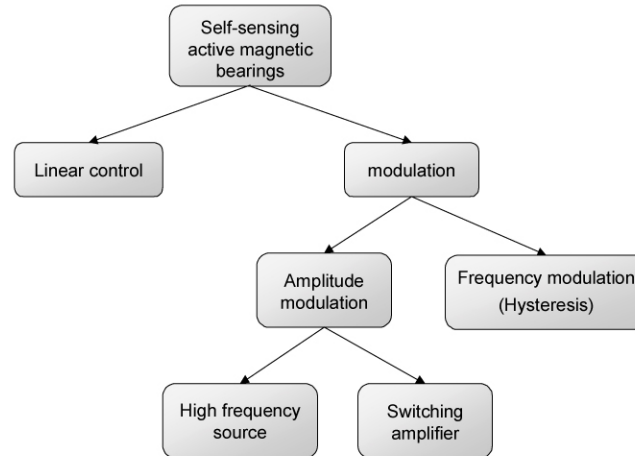


Figure 1: Types of self-sensing active magnetic bearings.

The modulation approach [3] is based on measuring the change of inductance caused by the rotor displacement. This approach is divided in amplitude and frequency modulation (Figure 1). In amplitude modulation, a high-frequency voltage signal is superposed to the control signal. In place of the high-frequency source, a PWM switching amplifier [4, 5, 6] can also be used. The current ripple amplitude depends on the coil inductance. Since the inductance depends on the air gap, the current is demodulated in order to estimate the position. In frequency modulation, a hysteresis switching amplifier is used. This type of amplifier uses a hysteresis comparator to control the switching times [7]. Since the switching frequency depends on the load impedance, the frequency changes with the rotor position. The change in frequency is then measured by a PLL.

## 3 Modeling

### 3.1 Coil

A simplified magnetic bearing coil can be modeled as illustrated in Figure 2. In the modeling, it is assumed that the behavior of the material is linear with constant permeability and no saturation. It is also considered that there is no flux leakage, and no eddy current losses. Applying Faraday's law to coil one, equation (1) is obtained:

$$u = n \frac{d\phi}{dt} + Ri \quad (1)$$

where  $u$  is the voltage across the coil,  $n$  represents the number of turns in the coil,  $\phi$  is the magnetic flux,  $R$  is the electrical resistance, and  $i$  is the current in the coil. Using Ampere's law, gives:

$$ni = l_m H_m + 2(x_0 - x)H_g \quad (2)$$

where  $l_m$  is the total core length,  $x$  is the rotor displacement with respect the nominal air gap  $x_0$ ,  $H_m$  and  $H_g$  represent the magnetic induction of the material and the gap respectively.

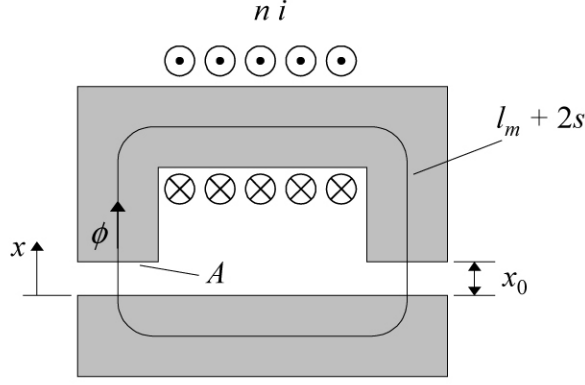


Figure 2: Simplified coil model.

Considering homogeneous distribution of flux and linear magnetic behavior, the current  $i$  can be derived from equation (2):

$$i = \frac{1}{n\mu_0 A} \left( 2(x_0 - x) + \frac{l_m}{\mu_r} \right) \phi \quad (3)$$

where  $\mu_0$  is the magnetic permeability,  $A$  is the cross section, and  $\mu_r$  is the relative permeability of the core material. Substituting  $\phi$  of equation (3) into equation (1), a relation among the current, voltage, and gap is obtained:

$$u = K \frac{d}{dt} \left( \frac{i}{2(x_0 - x) + \frac{l_m}{\mu_r}} \right) + Ri \quad (4)$$

where  $K = \mu_0 n^2 A$  is the magnetic bearing constant.

### 3.2 PWM Switching Amplifier

In the modulation approach, the actuator coils are fed by a switching amplifier. Figure 3 illustrates the operation principle of the three-state PWM amplifier used in this work. The voltage of each coil terminal is controlled separately by a pair of switches. The switches 1 and 2 control the voltage  $u_a$  and the switches 2 and 4 control the voltage  $u_b$ . The voltage  $u_a$  is switched between zero and the supply voltage  $u_z$  with a variable duty-cycle  $\alpha$ . In this case,  $\alpha=0$  represents  $u_a=0$ , and  $\alpha=1$  means  $u_a=u_z$ . In the other terminal, the voltage  $u_b$  is switched with constant duty-cycle of 50%. In this way, the control voltage across the coil  $u$  (the difference  $u_a - u_b$ ) presents an average between  $-u_z/2$  and  $u_z/2$ .

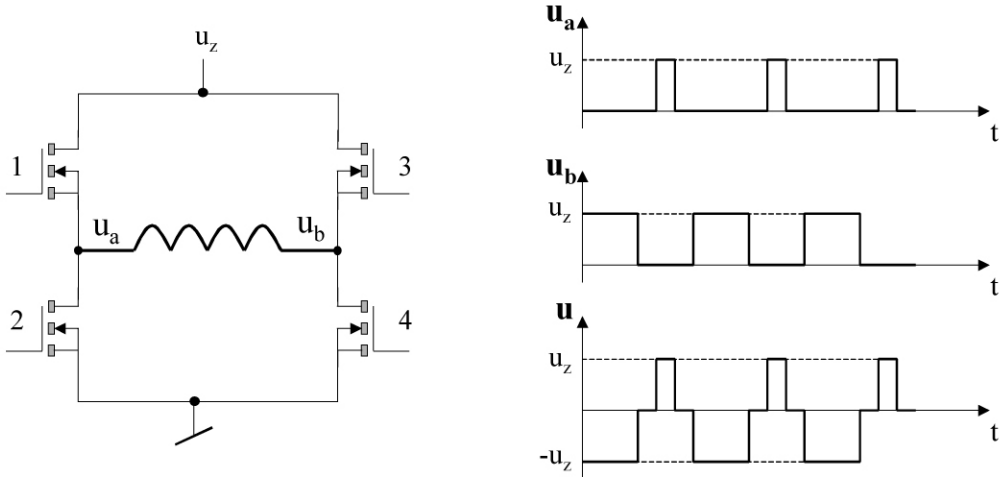


Figure 3: Three-state PWM switching amplifier.

This type of PWM amplifier circuit presents an advantage for self-sensing modulation compared to conventional two-state amplifiers [5]. Since the voltage  $u_b$  has a constant duty-cycle and phase shift of  $180^\circ$  with respect to  $u_a$ , the voltage ripple across the coil is never zero. This is true even at zero average control voltage. Since the proposed approach is based on the voltage and current ripple measurements, this amplifier set up guarantees that the position can be always estimated.

The voltage across the coil  $u$  can be approximated by Fourier series if the change of the duty-cycle is much slower than the switching frequency  $\omega_s$  [6]. Truncating the Fourier series at the first harmonic, equation (5) is obtained:

$$u(t) \cong u_z(\alpha - 0.5) + \frac{2u_z(1 + \sin \pi\alpha)}{\pi} \sin \omega_s t \quad (5)$$

## 4 Modulation Approach

The position must now be estimated based on the amplitude modulation described above. The major challenge of this approach is to obtain a sufficiently reliable, fast and clean position information out of the current measurement. Figure 4 illustrates the self-sensing approach and the position estimation algorithm. The figure describes the bearing coil driven by a PWM amplifier. The voltage and current are measured and the estimation algorithm calculates the position of rotor. This estimated position is used to stabilize the rotor position just in the same way as in a conventional system with sensors. The idea of this approach is based on the change of coil reluctance in function of gap.

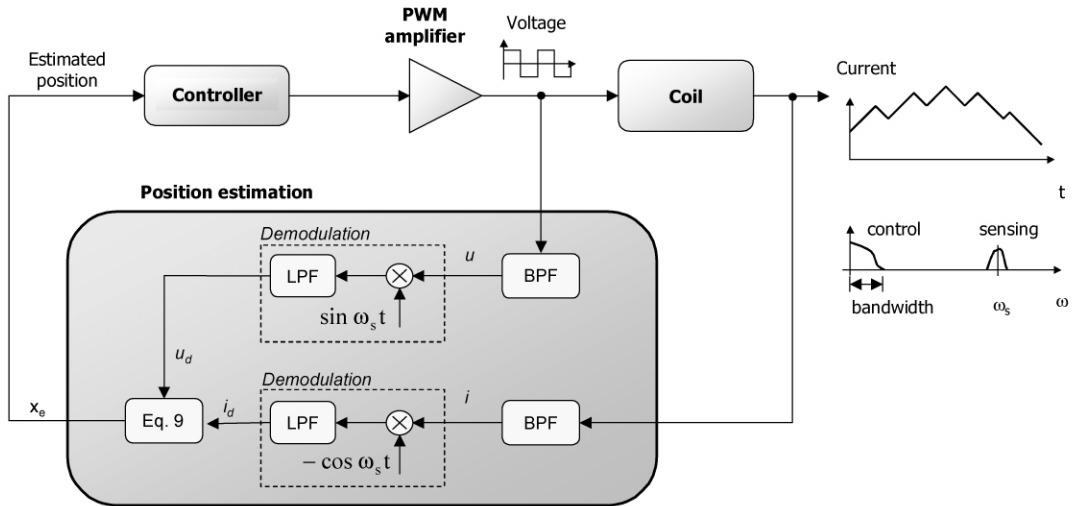


Figure 4: Estimation algorithm based on modulation approach.

As shown in equation (5), the amplifier voltage is composed of a low-frequency component that controls the rotor position and a ripple with frequency  $\omega_s$ . Considering  $\omega_s$  much higher than the control voltage bandwidth, it is assumed that control and sensing components are decoupled. For this purpose, the switching frequency must be selected sufficiently high above the control bandwidth, in practice higher than 10kHz.

It is shown in equation (5) that voltage ripple amplitude depends on the PWM duty-cycle. For this reason, the effect of voltage must be compensated in order to estimate the position accurately. The components of voltage and current carrying the position information are obtained by filtering the signals with a band-pass filter. Assuming that for high frequencies  $u \gg Ri$ , the current of the coil can be written:

$$i \cong \frac{1}{K} (-2x + s_0) \int u dt \quad (6)$$

where  $s_0 = 2x_0 + l_m / \mu_r$ . The band-pass filter is selected in such way as to obtain only the first harmonic of the voltage  $u$  at the switching frequency  $\omega_s$ :

$$u = \hat{u} \sin \omega_s t \quad (7)$$

where  $\hat{u} = 2u_z(1 + \sin \pi\alpha) / \pi$ . Assuming that bandwidth of  $\hat{u}$  is much smaller than the switching frequency  $\omega_s$ ,  $u$  can be substituted in equation (7) and gives:

$$i = -\frac{(-2x + s_0)}{K\omega_s} \hat{u} \cos \omega_s t \quad (8)$$

To obtain the amplitudes of the current  $i$  and voltage  $u$ , both signals are demodulated. As shown in Figure 4, synchronous demodulation is used in order to obtain the real part of demodulated current  $i_d$  and voltage  $u_d$ . The synchronous demodulation consists of multiplying the signal by a sinusoid with same phase (real demodulation). In this way, the estimated position  $x_e$  is obtained as follows:

$$x_e = \frac{1}{2} \left( -K\omega_s \frac{i_d}{u_d} + s_0 \right) \quad (9)$$

As it was explained in Section 2, the PWM amplifier setup guarantees that the division in equation (9) is well conditioned ( $u_d$  is never zero).

## 5 Results

Experimental results of a radial bearing are presented in this section. The quality of the estimation signal is discussed in terms of noise and dynamic performance.

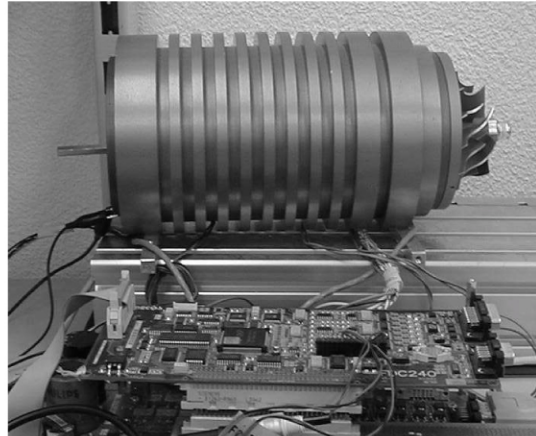


Figure 5: Test rig.

Figure 5 shows the test rig used for the experimental measurements. The system is composed of two radial bearings, one axial bearing and a short rotor with first bending mode of 1.5 kHz. The main characteristics of the system are the nominal air gap of 0.4 mm, and the maximum current of 1.2 A. The rotor has the length of 235 mm, and the weight of 2.78 kg. The switching frequency of PWM amplifier was 20 kHz.

As a typical AMB system, the test rig has two opposite coils for each axis [8]. Since both coils are influenced by the same change of rotor position, the current ripple of each coil was used to estimate the position. The objective of using the information of opposite coils is to increase robustness, with respect to noise, and modeling errors.

The position estimation algorithm was applied to one radial axis (one degree of freedom). Measurements in time and frequency domain were realized in order to evaluate the algorithm performance. The estimated position was compared to the measured position obtained from a reference sensor. The reference sensors used on the test rig were eddy current type.

Figure 6 shows the step response for a given desired position. The estimated and measured positions are compared. The estimated signal presents a small error with respect to the measured signal. The largest error is observed in the beginning of the step response, but it remains lower than 5% of the nominal gap. The measured noise of estimated position was relatively low. The measured peak-to-peak value was 3.7  $\mu\text{m}$ , which represents 1.5% of the nominal gap. This value is similar to the noise of measured position.

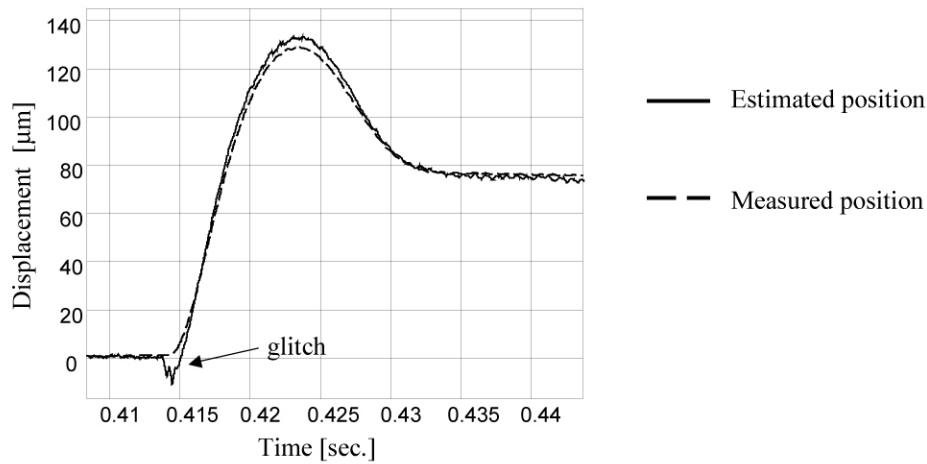


Figure 6: Step response of estimated and measured position.

Figure 7 shows the frequency response of the estimated position with respect to the measured position. This measurement is realized by feeding a constant sine-input to the controller. Since it is desired to have the estimated signal equal to the “true” position, ideally the frequency response would have magnitude one and phase zero.

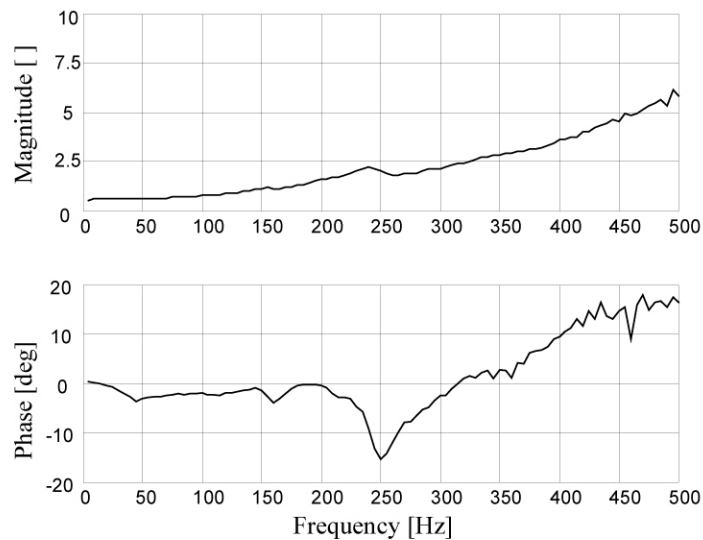


Figure 7: Frequency response of estimated position with respect to the sensor position.

The figure shows that the response well behaved is for low frequencies. However, for frequencies above ca. 100Hz, the phase remains small and the magnitude increases drastically. Additionally, further investigations have shown that the magnitude depends on the excitation amplitude.

## 6 Summary and Outlook

A self-sensing algorithm was presented based on modulation approach. Measurements in time and frequency domain were presented in order to evaluate the quality of estimated signals.

It was possible to float one axis of an AMB without sensors with relative low noise. The results show that estimated position has an excellent match with the “true” position and low noise for the frequency range of 100Hz. However, the quality of signal decreases for high frequencies.

To improve the dynamic performance, the next step is to refine the coil model. To achieve this, the material non-linearity must be investigated.

## 7 References

- [1]. D. Vischer. *Sensorlose und Spannungsgesteuerte Magnetlager*, Diss. Nr. 8665, ETH Zurich, 1988.
- [2]. D. Vischer, H. Bleuler. *Self-sensing Magnetic Levitation*, IEEE Transactions on Magnetics, v.29, n.2, pp.1276-1281, march 1993.
- [3]. L. Kučera. *Zur Sensorlosen Magnetlagerung*, Diss, Nr. 12249, ETH Zurich, 1997.
- [4]. Y. Okada, K. Matsuda, B. Nagai. *Sensorless Magnetic Levitation Control by Measuring the PWM Carrier Frequency Component*, in Proceedings of Third International Symposium on Magnetic Bearings, pp. 176-183, 1992.
- [5]. D. T. Montie, E. H. Maslen. *Experimental Self-Sensing Results for a magnetic bearing*, in Proceedings of Seventh International Symposium on Magnetic Bearings, 2000.
- [6]. M. D. Noh. *Self-Sensing Magnetic Bearing Driven by a Switching Power Amplifier*, Phd. thesis, University of Virginia, 1996.
- [7]. T. Mizuno, T. Ishii, K. Araki. *Self-Sensing Magnetic Suspension Using Hysteresis Amplifiers*, in Proceedings of Fifth International Symposium on Magnetic Bearings, pp. 1133-1140, 1998.
- [8]. G. Schweitzer, H. Bleuler, A. Traxler. *Active Magnetic Bearings: Basics, Properties and Applications of Active Magnetic Bearings*, Verlag der Fachvereine, Zurich, Switzerland, 1994.